Fusion imaging for EVAR with mobile c-arm

Adrien Kaladji, Alexandre Villena, Remy Pascot, Florent Lalys, Anne Daoudal, Elodie Clochard, Antoine Lucas, Alain Cardon

Original article

Fusion imaging for EVAR with mobile c-arm

Adrien Kaladji[1,2,3], Alexandre Villena[1], Remy Pascot[1], Florent Lalys[4], Anne Daoudal[1], Elodie Clochard[1], Antoine Lucas[1,2,3], Alain Cardon[1]

1. Rennes University Hospital, Centre of Cardiothoracic and Vascular Surgery, F-35033 Rennes, France
2. INSERM, U1099, F-35000 Rennes, France
3. University Rennes 1, Signal and Image Processing Laboratory (LTSI), F-35000 Rennes, France
4. Therenva, F-35000, Rennes, France

Corresponding author:

Adrien Kaladji, Centre of Cardiothoracic and Vascular Surgery, Rennes University Hospital, F-35033 Rennes, France

kaladrien@hotmail.fr

Word count : 2575

ABSTRACT

Introduction

Fusion imaging is a technique that facilitates endovascular navigation but is only available in hybrid rooms. The goal of this study was to evaluate the feasibility of fusion imaging with a mobile C-arm in a conventional operating room through the use of an angio-navigation station.

Methods

From May 2016 to June 2017, the study included all patients who underwent an aortic stent graft procedure in a conventional operating room with a mobile flat-panel detector (Cios Alpha, Siemens) connected to an angio-navigation station (EndoNaut, Therenva). The intention was to perform preoperative 3D CT/perioperative 2D fluoroscopy fusion imaging using an automatic registration process. Registration was considered successful when the software was able to correctly overlay preoperative 3D vascular structures onto the fluoroscopy image. For EVAR, contrast dose, operation and fluoroscopy time were compared to those of a control group drawn from the department's database who underwent a procedure with a C-arm image intensifier.

Results

The study included 54 patients and the procedures performed were: 49 EVAR, 2 TEVAR, 2 IBD, 1 FEVAR. Of the 178 registrations that were initialised, it was possible to use the fusion imaging in 170 cases, i.e. a 95.5% success rate. In the EVAR comparison, there were no difference with the control group (n=103) for fluoroscopy time (21.9 ± 12 vs. 19.5 ± 13 min, p=0.27), but less contrast agent was used in the group undergoing a procedure with the angio-navigation station (42.3 ± 22 ml vs. 81.2 ± 48 ml, p<0.001) and operation time was shorter (114 ± 44 vs. 140.8 ± 38 min, p<0.0001).

Conclusion

Fusion imaging is feasible with a mobile C-arm in a conventional operating room and thus represents an alternative to hybrid rooms. Its clinical benefits should be evaluated in a randomised series but our study already suggests that EVAR procedures might be facilitate with an angionavigation system.

Key words: Fusion imaging; mobile c-arm; flat panel; EVAR; hybrid room; registration

Introduction

Fusion imaging is a technique used in vascular surgery in which a preoperative 3D CT scan is projected onto 2D fluoroscopy. This makes it possible to navigate the vascular tree without necessarily having to use iodinated contrast agent. An increasing number of studies are reporting on the use of fusion imaging in aortic endovascular procedures and its benefits(1-5). This imaging modality is however based on a certain number of prerequisites that limit the number of centres using it. These prerequisites are currently only fulfilled by floor-mounted fixed imaging systems that make automatic adjustments for movements of the operating table. Fusion imaging involves alignment (registration) of the preoperative CT scan with the fluoroscopy image. Once registration has been performed, whenever the table or C-arm moves the system is capable of realigning the preoperative CT scan with the 2D fluoroscopy image. In practice, only surgeons performing procedures in hybrid rooms have access to fusion imaging and other modern navigation tools. The cost of hybrid rooms is a major barrier to adoption of this technique.

The FUTUR study (whose French acronym stands for 'feasibility of computer-assisted aortic and iliac endovascular procedures with mobile C-arm') set out to overcome the challenge of performing fusion imaging with a mobile C-arm in a conventional operating room and making it compatible with the clinical workflow.

Patients and Methods

The protocol and informed consent form were approved by the local institutional review board, and all subjects gave informed consent.

Study design

The study was a single-centre, prospective, consecutive feasibility pilot study. The primary

objective was to evaluate the feasibility of fusion imaging during aortic endovascular procedures with a mobile C-arm through the use of the EndoNaut® angio-navigation station (Therenva; Rennes, France). Secondary objectives were to evaluate the efficiency of the system when deploying infrarenal aortic stent grafts to treat unruptured atheromatous aneurysms (EVAR).

The primary endpoint was the feasibility rate of fusion defined as the convergence of bone registration and the projection of the vascular 3D structure onto the fluoroscopy image (number of initialised registrations/number of convergent registrations). If the accuracy and robustness of the registration algorithm was already quantified in Duménil et al. (20), the convergence of the algorithm was qualitatively performed by visual inspection of the main angio-navigation system user solely. Registration failures were easily detectable even from a non-expert eye as the algorithm gave an aberrant solution to the registration problem. Secondary endpoints concerned radiation dose as measured by fluoroscopy time (FT in min), dose-area product (DAP in $Gy.cm^2$) and air kerma (AK in mGy).

Inclusion criteria

Patients eligible for endovascular treatment of aneurysm disease of the aorta.

Procedure performed in a conventional operating room equipped with a mobile flat-panel detector (30×30 cm) (Cios-Alpha, Siemens®, Munich, Germany) and a floating table.

Patients who received written and verbal information about the protocol and did not object to participating in the trial.

Non-inclusion criteria

-Patients who also required a conventional surgical revascularisation procedure or who required an endovascular revascularisation procedure in another site.

-Patients who underwent MR angiography during preoperative evaluation.

-Non-analysable CT angiogram (no or poor injection).

-Procedure performed in a hybrid room or in an operating room not equipped with a mobile flat-panel detector.

Fusion imaging principle and operation of EndoNaut® station

The EndoNaut station is connected to the C-arm and retrieves the video signal generated by the C-arm (Fig. 1). The station is positioned in front of the surgeon and becomes his or her primary navigation interface. Sizing and planning data are derived from the preoperative analysis carried out with EndoSize® software (Therenva; Rennes, France) and transmitted to the station by importing a dedicated file from a USB storage device. The following data are exported from the sizing software: aortoiliac mesh with key points used for sizing represented as rings (below the lowest renal artery, iliac bifurcations – Fig. 1). All measurements and aortic 3D screenshots (reporting c-arm angulation) are also exported. Human-computer interaction is via a touch-sensitive tablet in one touch mode. Preoperative CT-scan is searchable during all the procedure thanks to the tablet which controls every “image action” (registration, navigation, measurements, numerical zoom...). To use fusion imaging functionality, the registration must be initialised after setting C-arm/operating table angulation as determined during preprocedural planning. The user then has to align, in an approximate manner and in only one view, the bone 3D volume of the preoperative CT scan with the 2D bony structures of the fluoroscopy image. Next, the software performs perfect, precise alignment of bony structures using rigid 3D/2D registration. The duration of this geometric transformation depends on the size of the image matrix and the C-arm used. For the C-arm used in the present study, the average duration was 15 +/- 3s and never exceeded 22 seconds. Each registration is valid until either the table or the C-arm position/angulation (i.e. C-arm

pose) changes. A new registration becomes mandatory in that cases, and on the contrary to fixed C-arm in hybrid room the fusion mask cannot be used to automatically position the table or the gantry. After completion of registration, the vascular tree is projected with the planning data defined using EndoSize®. Rings are visible in the planned deployment areas in the upper and lower landing zones (Fig. 2A). For tortuous anatomy, in order to anticipate anatomical deformations(6-8) caused by the extrastiff guidewire and the delivery system, a previously simulated deformed 3D model is projected (Fig. 2B). Several studies have specifically addressed simulation(9-11). These simulations are not carried out by the station but on a workstation dedicated to sizing and simulation. For TEVAR (thoracic stentgrafts), FEVAR (fenestrated stentgrafts) and IBD procedures (iliac branched device), rings are projected onto the planned landing zones and the ostia of target vessels (Fig. 3 and 4). The precision of the fusion in terms of location of target vessels (renal, internal iliac arteries) is always verified by injection of a small volume of iodinated contrast agent. If there is a misalignment of the projection of the 3D fusion mask and angiography due to the insertion of stiff guidewire, adjustments are made.

Control group

For the EVAR procedures, contrast dose, fluoroscopy an operation time were compared to those of a control group of patients who received an aorto-bi-iliac stent graft for non-ruptured AAA using a mobile image intensifier system (OEC 9800, General Electric; GE, USA) without an angionavigation station. These patients were drawn from the local EVAR database and were operated upon between January 2013 and December 2014, the date on which the mobile flat-panel detector in the study came into use.

Statistical analysis

153 Quantitative data are expressed as mean ± standard deviation and qualitative data as a number
154 and corresponding percentage. Data were compared using Student's t-test. Significance was
155 set at $p<0.05$.
156

Results

Patients and procedures

From 1 May 2016 to 30 June 2017, 54 patients (49 men, 92.6%) of mean age 73.4 ± 9.3 years were included in the study. Mean BMI was 28.3 ± 7.7 kg/m^2. The procedures performed were: 49 bifurcated stent grafts including 2 with unilateral internal iliac artery embolisation and one with an anchoring system (Aptus, Medtronic); 2 branched iliac; 2 thoracic; and 1 fenestrated stent graft. The mean duration of the EVAR procedures was 103.6 ± 25.4 min. In this cohort, proximal and distal seals were achieved with the successful introduction and deployment of the device in the absence of surgical conversion or mortality, type I or III endoleaks, or graft limb obstruction. Considering this definition, the technical success was 100%. Percutaneous access was performed for 50 (92.6%) patients (bilateral) without open conversion by using 6 Fr Perclose Proglide device (Abbott Vascular, Redwood City, CA). Every percutaneous access was ultrasound-guided. Patients were deemed unfit for percutaneous access (n=4) when the majority of the anterior wall of the common femoral arteries were calcified.

Primary endpoint

The mean number of registrations initialised per patient was 3.3 ± 1.1. Of the 178 registrations initialised across all patients, it was possible to project the vascular tree onto fluoroscopy in 170 cases, i.e. a feasibility rate of 95.5%. The feasibility rate seems to be similar for all procedure types (Table 1).

Secondary endpoints and comparison with control group

Table 1 shows the radiation and contrast dose for each procedure type. The control group consisted of 103 patients who underwent EVAR (Fig. 4). Demographic data are compared

between the EVAR group of the FUTUR study and the control group in the table 2. For radiation data, no significant difference between the groups was found. On the basis of comparable body mass indices, fluoroscopy time (21.9 ± 12 vs. 19.5 ± 13 min, p=0.27) and dose-area product (70.6 ± 48 vs. 67.3 ± 74 Gy.cm^2, p=0.77) did not vary between the two groups. However, less contrast agent was used in the "FUTUR" group (42.3 ± 22 ml vs. 81.2 ± 48 ml, p<0.0001).

Discussion

Herein we report what is to our knowledge the first use of software capable of performing 3D monomodal (CT)/2D fusion with a mobile C-arm for the placement of an aortic stent graft. In all series reporting the use of fusion imaging a fixed system has been necessary(1, 3, 12-19). The main reason is that the operating table has to be connected to the imaging system so that the latter can realign the preoperative CT scan with the fluoroscopy image whenever the table moves. In this regard, the system we report is not capable of realignment and this may constitute in itself a limitation. However, in routine practice, fusion imaging is only useful at very specific moments during placement of, for example, a bifurcated stent graft. During deployment of the main body, the angle of the C-arm has already been determined in advance, and the practitioner can focus on gradual deployment of the stents and needs to see the position of the renal arteries to perfectly position the stent graft. At this stage, there are no table or C-arm movements; on the contrary, good visualisation of the stent graft and aorta is required. This is also true during deployment of the iliac limbs, in order to ensure precise placement in relation to the internal iliac artery. During insertion of the guidewire, catheters or stent graft, and even during catheterisation of the contralateral stump, table movements are frequent, but projection of the vascular tree is not essential to the practitioner. So although the

software reported here requires that registration be repeated after every table movement, in our opinion this does not constitute a limitation in routine practice.

The technological challenge presented by fusion imaging with a mobile C-arm is to offer registration that is as fast as possible and above all only requires one 2D fluoroscopy view so that the system is compatible with the clinical workflow. The EndoNaut® station is the only software that uses only one 2D view to perform registration with the 3D CT scan, as has been previously reported(20). If the current system only uses information extracted from the pre-operative 3D CT scan, other types of imaging modalities (MRI, non-enhanced CT, ultrasound) could also be considered and is a subject of further improvement. The first publications for fusion imaging described systems that could only perform 3D/3D registration, which required CBCT at the start of the procedure(19, 21, 22). Given the radiation emitted by CBCT, systems evolved towards 3D/2D registration(3) that restricted CBCT to post-procedure assessment(23-26). Hence 2D fluoroscopy acquisition was necessary but 2 views were needed to achieve sufficient precision and this is no longer the case in the present study. With regard to the duration of the registration calculation, we did not report it in a quantitative manner because short duration is a prerequisite for studies such as the present one designed to demonstrate feasibility before envisaging studies to demonstrate clinical benefits. The reported results demonstrate that fusion imaging is feasible in the vast majority of EVAR cases. It was not feasible in cases with C-arm/operating table procedural angulations that were extreme for a conventional operating room. Beyond 35-40° inclination (regardless of orientation), the fluoroscopy image is contaminated by bony structures such as the upper limbs which are not visible on the CT scan and which jeopardize alignment of the two reference images. Nevertheless, this problem can be overcome by abducting and externally rotating the arms during the procedure, for example.

The majority of patients in our study underwent EVAR, as this is the predominant activity and it is also the procedure with the highest reproducibility. The other stent graft cases we reported are anecdotal and were mentioned in order to demonstrate that the station also works with other procedures. Similarly, we did not report cases of iliac recanalization or renal and mesenteric angioplasty, which are now systematically performed with the station.

Unsurprisingly, the radiation dose was not shown to be lower than in the control group. This finding must be interpreted with the utmost caution because the comparison involves completely different systems. The flat-panel detector does not use the same technology as an image intensifier, nor does it have the same physical characteristics, both factors that affect the delivered dose. Hence, drawing conclusions from this finding is fraught with bias.

Moreover, we are reporting the experience of one teaching hospital, one in which experienced senior practitioners, senior practitioners who have become independent more recently and junior practitioners under supervision participate in procedures. There is heterogeneity in the use of X-rays beyond adherence to ALARA principles. For example, a junior practitioner will attempt to track progress of the device through the aorta fluoroscopically, whereas a senior practitioner will insert the device "blindly". The real comparison for radiation dose and X-ray use would be a single-operator randomised series to overcome the anatomical differences between patients that give rise to procedural difficulties. In comparison to image intensifiers, flat-panel detectors offer higher image quality (more pixels per mm^2), and the image matrix is larger, so a higher radiation dose could have been expected, but this was not the case.

On the other hand, when we consider use of contrast agent, there is a clear difference. And it is more logical to consider that the benefit is related to the station and not to the different characteristics of the C-arms used. As a reminder, in the series of Hertault et al.(3), use of a hybrid operating room did not lead to a significant reduction in the volume of contrast agent used for bifurcated stent grafts (only for fenestrated/branched stent grafts). In this series, the

X-ray dose reduction was very clear but it was comparing two different systems, hence it was not the fusion imaging that led to this reduction.

Finally, the recent meta-analysis by De Ruiter et al.(4) concluded: "For equivalent fluoroscopy times, the use of a fixed C-arm in noncomplex procedures leads to higher patient radiation doses compared to a mobile C-arm". We therefore believe that the combination of a mobile flat-panel detector with fusion imaging is a completely acceptable alternative to a hybrid operating room.

Limitations

In the present study, we did not report any quantitative criteria for fusion precision. Several publications(2, 6, 8, 12) have shown that, regardless of the registration method used, fusion precision is found to be lacking when compared to subtraction angiography. Maurel et al.(6) clearly showed, with the aid of perioperative CBCT, displacement of the ostia of renal and visceral arteries in different planes due to deformations caused by insertion of a rigid material (extrastiff guide, introducer) in the aorta. Several solutions have been considered to resolve this phenomenon, such as "Image-based tracking fusion system" approaches. We decided not to measure fusion precision here because currently no system is able to predict deformations in a very precise manner. Even in cases with non-tortuous anatomy, there may be a mismatch between the fused image and angiography, which in our opinion remains essential for validating the fusion (7 ml to 30 ml/s suffice at the proximal landing zone). As long as registration is based on bony structures (hence with rigid transformations), there will be a mismatch with arterial structures which by nature are soft and deformable, which therefore calls for approaches based on elastic registration(27), for example, or digital simulation approaches that predict deformations using a biomechanical model. We have already published several studies on this simulation approach(10, 11), which is integrated into the

planning and fusion software. The objective of the present study was not to test the precision of registration with a simulated and deformed model. A specific methodology, which was not possible nor envisaged in the study design, needs to be developed for this purpose (using, among others, perioperative CBCT). Moreover, we have already quantified the accuracy and robustness of the registration algorithm in the dedicated methodological article presenting the detailed principle of the 3d/2d registration (20). In this already published paper, a thorough and precise validation scheme was proposed, and the mean registration error on the bony landmarks was found to be < 0.5mm. Finally, the learning curve of the team and the fact that we are a training center can lead to a bias in the reproducibility of the results and the efficiency in the EVAR procedures. In this study, there was investigators with different experiences (range from 10 to 300 EVAR procedures) but subgroups would not give enough statistical power to reach statistical differences in radiation parameters.

Conclusion

Fusion of the 3D preoperative CT scan with 2D fluoroscopy is possible with a mobile C-arm and compatible with the clinical workflow. In addition to the unquantifiable visual comfort and the possibility of using all modern navigation tools, this technique also appears to reduce the volume of contrast agent for EVAR procedures. The combination of a mobile flat-panel detector with a computer-assisted surgery station is an acceptable alternative to hybrid operating rooms for complex aortic procedures with high-performance imaging.

Conflict of interest

no

Funding

None

Acknowledgements

References

1. Dias NV, Billberg H, Sonesson B, Tornqvist P, Resch T, Kristmundsson T. The effects of combining fusion imaging, low-frequency pulsed fluoroscopy, and low-concentration contrast agent during endovascular aneurysm repair. J Vasc Surg 2016;63:1147-55.

2. Tacher V, Lin M, Desgranges P, Deux JF, Grunhagen T, Becquemin JP, *et al.* Image guidance for endovascular repair of complex aortic aneurysms: comparison of two-dimensional and three-dimensional angiography and image fusion. J Vasc Interv Radiol 2013;24:1698-706.

3. Hertault A, Maurel B, Sobocinski J, Martin Gonzalez T, Le Roux M, Azzaoui R, *et al.* Impact of hybrid rooms with image fusion on radiation exposure during endovascular aortic repair. Eur J Vasc Endovasc Surg 2014;48:382-90.

4. de Ruiter QM, Reitsma JB, Moll FL, van Herwaarden JA. Meta-analysis of Cumulative Radiation Duration and Dose During EVAR Using Mobile, Fixed, or Fixed/3D Fusion C-Arms. J Endovasc Ther 2016;23:944-56.

5. Maurel B, Hertault A, Sobocinski J, Le Roux M, Gonzalez TM, Azzaoui R, *et al.* Techniques to reduce radiation and contrast volume during EVAR. J Cardiovasc Surg (Torino) 2014;55:123-31.

6. Maurel B, Hertault A, Gonzalez TM, Sobocinski J, Le Roux M, Delaplace J, *et al.* Evaluation of visceral artery displacement by endograft delivery system insertion. J Endovasc Ther 2014;21:339-47.

7. Kaladji A, Dumenil A, Castro M, Cardon A, Becquemin JP, Bou-Said B, *et al.* Prediction of deformations during endovascular aortic aneurysm repair using finite element simulation. Comput Med Imaging Graph 2013;37:142-9.

8. Kauffmann C, Douane F, Therasse E, Lessard S, Elkouri S, Gilbert P, *et al.* Source of errors and accuracy of a two-dimensional/three-dimensional fusion road map for endovascular aneurysm repair of abdominal aortic aneurysm. J Vasc Interv Radiol 2015;26:544-51.

9. Gindre J, Bel-Brunon A, Combescure A, Haigron P, Rochette M, Lucas A. Estimation of clinically relevant indicators for EVAR using patient-specific finite element simulation. Comput Methods Biomech Biomed Engin 2015;18 Suppl 1:1950-1.

10. Gindre J, Bel-Brunon A, Kaladji A, Dumenil A, Rochette M, Lucas A, *et al.* Finite element simulation of the insertion of guidewires during an EVAR procedure: example of a complex patient case, a first step toward patient-specific parameterized models. Int J Numer Method Biomed Eng 2015;31:e02716.

11. Gindre J, Bel-Brunon A, Rochette M, Lucas A, Kaladji A, Haigron P, *et al.* Patient-Specific Finite-Element Simulation of the Insertion of Guidewire During an EVAR Procedure: Guidewire Position Prediction Validation on 28 Cases. IEEE Trans Biomed Eng 2017;64:1057-66.

12. Sailer AM, de Haan MW, Peppelenbosch AG, Jacobs MJ, Wildberger JE, Schurink GW. CTA with fluoroscopy image fusion guidance in endovascular complex aortic aneurysm repair. Eur J Vasc Endovasc Surg 2014;47:349-56.

13. Kaladji A, Dumenil A, Castro M, Haigron P, Heautot JF, Haulon S. Endovascular aortic repair of a postdissecting thoracoabdominal aneurysm using intraoperative fusion imaging. J Vasc Surg 2013;57:1109-12.

14. Koutouzi G, Henrikson O, Roos H, Zachrisson K, Falkenberg M. EVAR Guided by 3D Image Fusion and CO2 DSA: A New Imaging Combination for Patients With Renal Insufficiency. J Endovasc Ther 2015;22:912-7.

15. Tacher V, Desgranges P, You K, Ridouani F, Marzelle J, Kobeiter H. Feasibility of Three-Dimensional MR Angiography Image Fusion Guidance for Endovascular Abdominal Aortic Aneurysm Repair. J Vasc Interv Radiol 2016;27:188-93.

16. Alomran F, Desgranges P, Majewski M, You K, Kobeiter H. Image fusion for hybrid repair of dislocated superior mesenteric branch of a branched endovascular aortic graft. J Vasc Surg 2013;58:798-801.

17. Kaladji A, Daoudal A, Clochard E, Gindre J, Cardon A, Castro M, *et al.* Interest of fusion imaging and modern navigation tools with hybrid rooms in endovascular aortic procedures. J Cardiovasc Surg (Torino) 2017;58:458-66.

18. Koutouzi G, Sandstrom C, Roos H, Henrikson O, Leonhardt H, Falkenberg M. Orthogonal Rings, Fiducial Markers, and Overlay Accuracy When Image Fusion is Used for EVAR Guidance. Eur J Vasc Endovasc Surg 2016;52:604-11.

19. Kobeiter H, Nahum J, Becquemin JP. Zero-contrast thoracic endovascular aortic repair using image fusion. Circulation 2011;124:e280-2.

20. Dumenil A, Kaladji A, Castro M, Goksu C, Lucas A, Haigron P. A versatile intensity-based 3D/2D rigid registration compatible with mobile C-arm for endovascular treatment of abdominal aortic aneurysm. Int J Comput Assist Radiol Surg 2016;11:1713-29.

21. Dijkstra ML, Eagleton MJ, Greenberg RK, Mastracci T, Hernandez A. Intraoperative C-arm cone-beam computed tomography in fenestrated/branched aortic endografting. J Vasc Surg 2011;53:583-90.

22. Kaladji A, Dumenil A, Mahe G, Castro M, Cardon A, Lucas A, *et al.* Safety and accuracy of endovascular aneurysm repair without pre-operative and intra-operative contrast agent. Eur J Vasc Endovasc Surg 2015;49:255-61.

23. Biasi L, Ali T, Hinchliffe R, Morgan R, Loftus I, Thompson M. Intraoperative DynaCT detection and immediate correction of a type Ia endoleak following endovascular repair of abdominal aortic aneurysm. Cardiovasc Intervent Radiol 2009;32:535-8.

24. Biasi L, Ali T, Ratnam LA, Morgan R, Loftus I, Thompson M. Intra-operative DynaCT improves technical success of endovascular repair of abdominal aortic aneurysms. J Vasc Surg 2009;49:288-95.

25. Hertault A, Maurel B, Pontana F, Martin-Gonzalez T, Spear R, Sobocinski J, *et al.* Benefits of Completion 3D Angiography Associated with Contrast Enhanced Ultrasound to Assess Technical Success after EVAR. Eur J Vasc Endovasc Surg 2015;49:541-8.

26. Tornqvist P, Dias N, Sonesson B, Kristmundsson T, Resch T. Intra-operative cone beam computed tomography can help avoid reinterventions and reduce CT follow up after infrarenal EVAR. Eur J Vasc Endovasc Surg 2015;49:390-5.

27. Nasr B, Le Ven F, Savean J, Ben Salem D, Nonent M, Gouny P, *et al.* Characterization of the Physiological Displacement of the Aortic Arch Using Non-Rigid Registration and MR Imaging. Eur J Vasc Endovasc Surg 2017;53:282-9.

Legends for figures and tables

Fig. 1: The angio-navigation station is placed in front of the surgeon (black arrow), who interacts with it via a remote touch-sensitive tablet (white arrow) providing all image-related actions (zoom, registration, CT scan interpretation, etc.). Screens of the c-arm are placed on the right (yellow arrow).

Fig. 2: Fusion of preoperative CT scan for EVAR using a non-deformed model (A), which is nullified by deformations caused by rigid tools. Adjustment of the fused image (B) by projection of a model deformed by digital simulation.

Fig. 3: Regardless of the procedure, low-volume angiography is systematically performed to verify the position of renal arteries in FEVAR procedures for example (A). The prosthesis is deployed under fusion imaging guidance (B) and catheterisation is performed without the roadmap (C).

Fig. 4: For TEVAR procedures in the descending thoracic artery, the prosthesis is deployed frontally (A). A ring is projected onto the distal landing zone and the coeliac trunk (B-C). This avoids a procedure with the C-arm sideways, which would increase the radiation dose to the operator.

Fig. 5: Box plots comparing variables of patients operated on with the angio-navigation station and the control group.

Table 1: Fusion feasibility rate and contrast and radiation dose by procedure type

	Registration success	Contrast agent (mL)	Fluoroscopy time (min)	DAP ($Gy.cm^2$)	AK (mGy)
EVAR (n=49)	95.1% (155/163)	41.9 ± 23.1	21.6 ± 12.3	70.9 ± 48.2	254.2 ± 161.5
TEVAR (n=2)	100% (4/4)	23.8	6	20	79
IBD (n=2)	100% (6/6)	39.8	39.8	67.7	363.5
FEVAR (n=1)	100% (5/5)	65	38	163.1	603

* DAP = Dose-area product, AK = Air kerma

Table 2

	EVAR Fusion (n=49)	EVAR No fusion (n=103)	*P* value
Age (years; mean ± SD)	73.7 ± 9.3	73.9 ± 9	0.89
Gender (Male)	44 (89.8%)	97 (94.2%)	0.26
BMI (kg/m^2)	28.3 ± 5	26.9 ± 4	0.19
Symptomatic PAD*	0 (0%)	4 (3.8%)	0.21
Coronary artery lesions	12 (24.5%)	28 (27.2%)	0.84
Severe respiratory failure	1 (2%)	4 (3.9%)	0.48
Renal failure (eGFR<30)**	2 (4.1%)	6 (5.8%)	0.49
Treated hypertension	30 (61.2%)	82 (79.2%)	0.06
History of tobacco	36 (73.5%)	75 (72.8%)	0.9
Diabetes	6 (12.2%)	7 (6.8%)	0.53
Treated dyslipidemia	35 (71.4%)	64 (62.1%)	0.53
Anticoagulant therapy	3 (6.1%)	4 (3.9%)	0.41

* Peripheral Arterial Disease

**Estimated Glomerular filtration Rate in ml/min/1.73m^{-2}

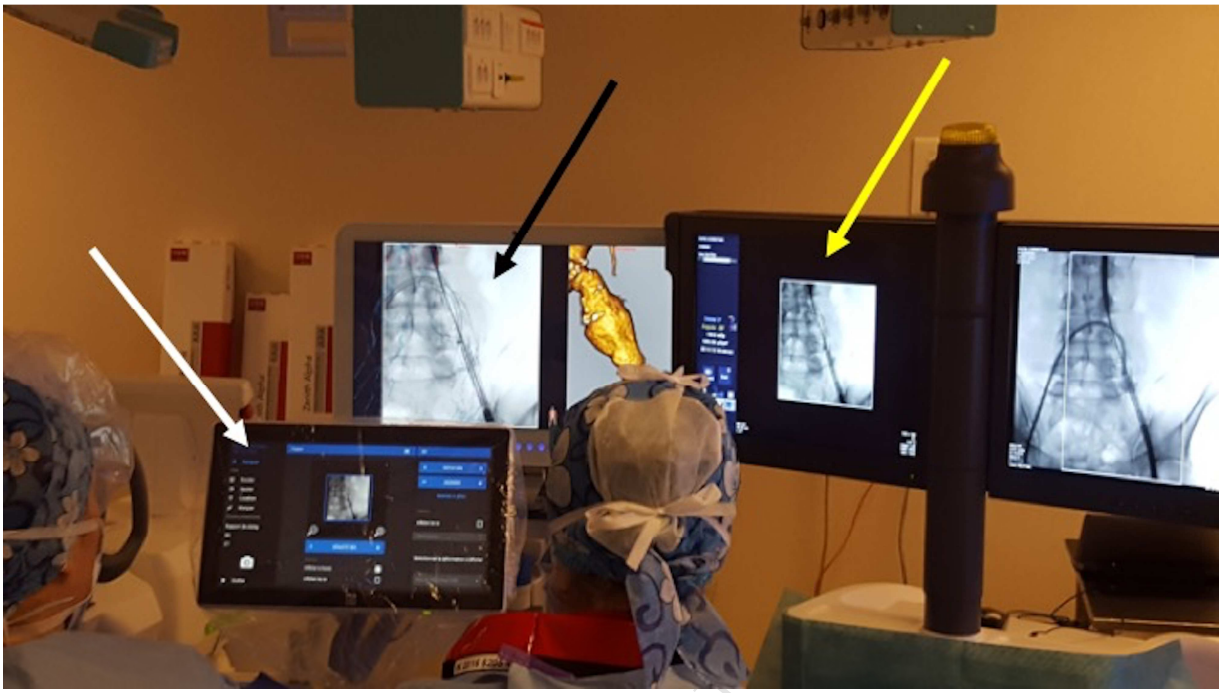

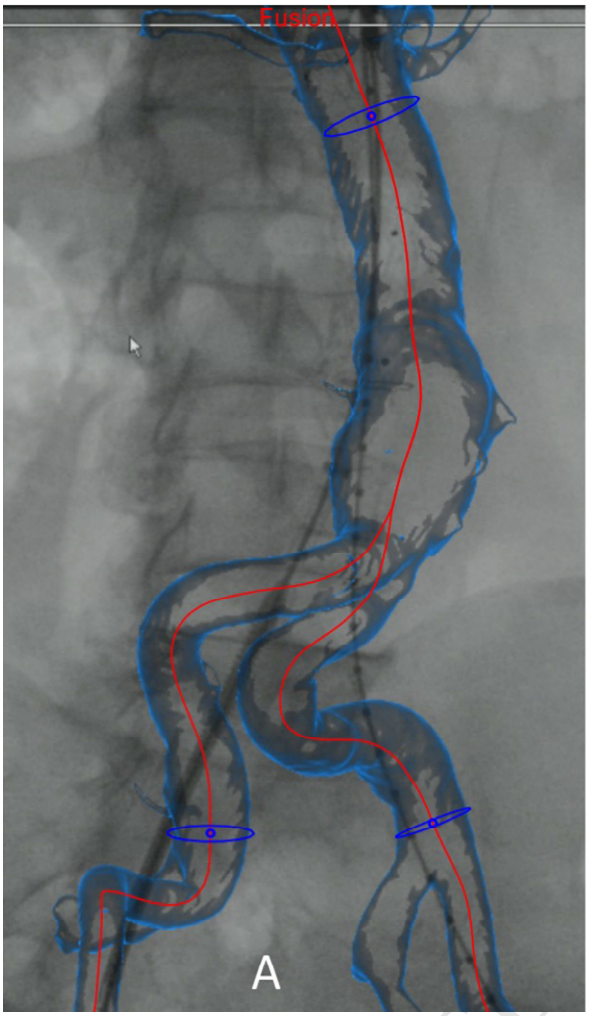

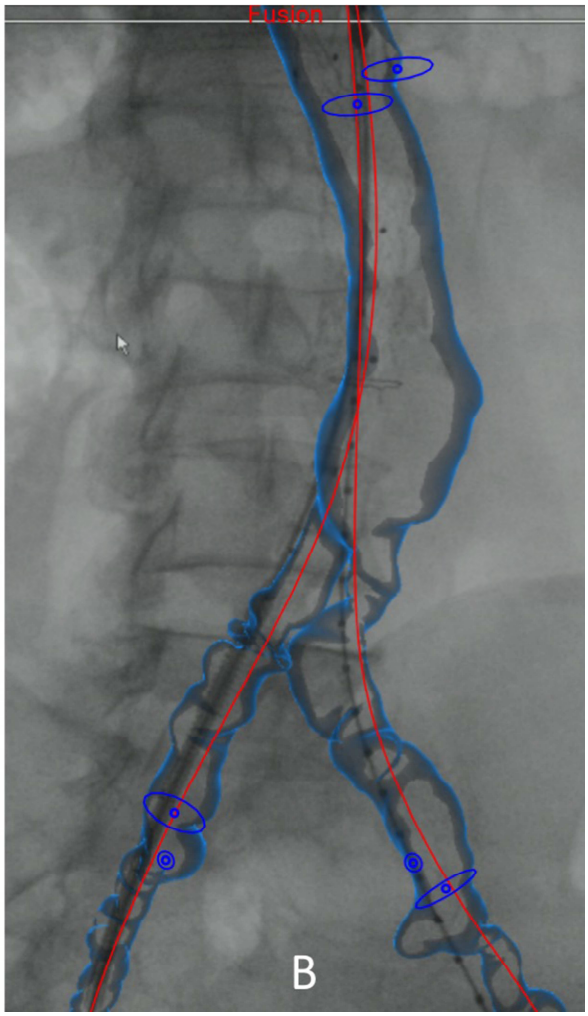

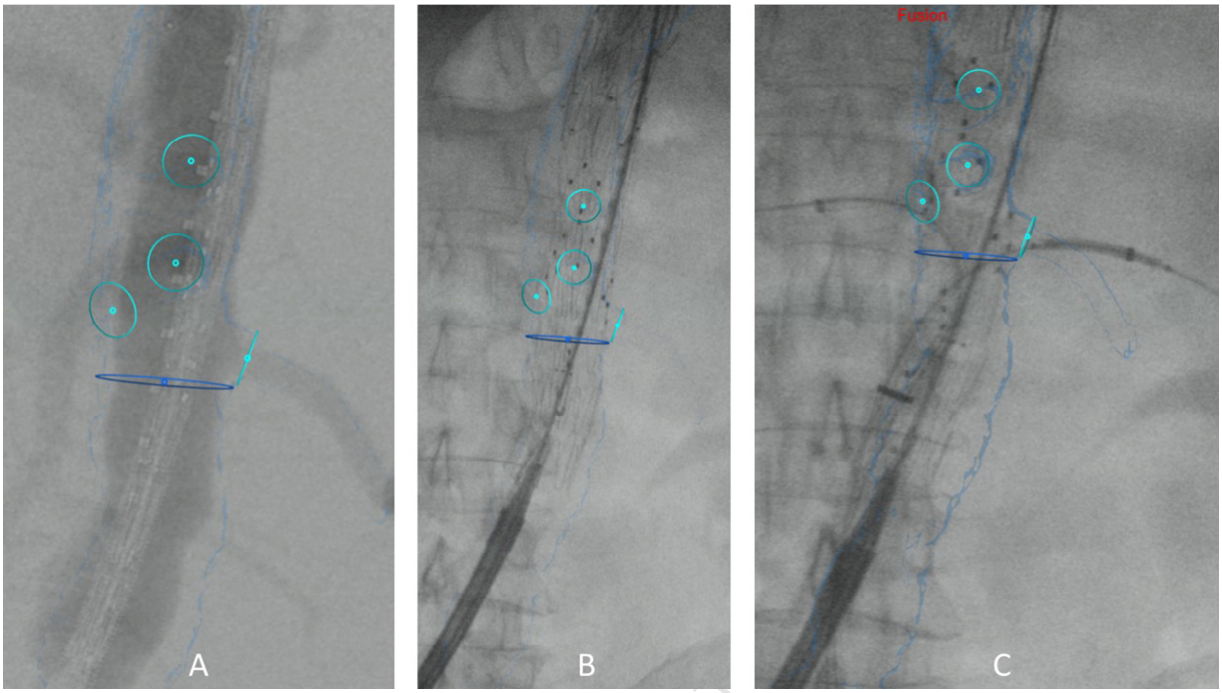

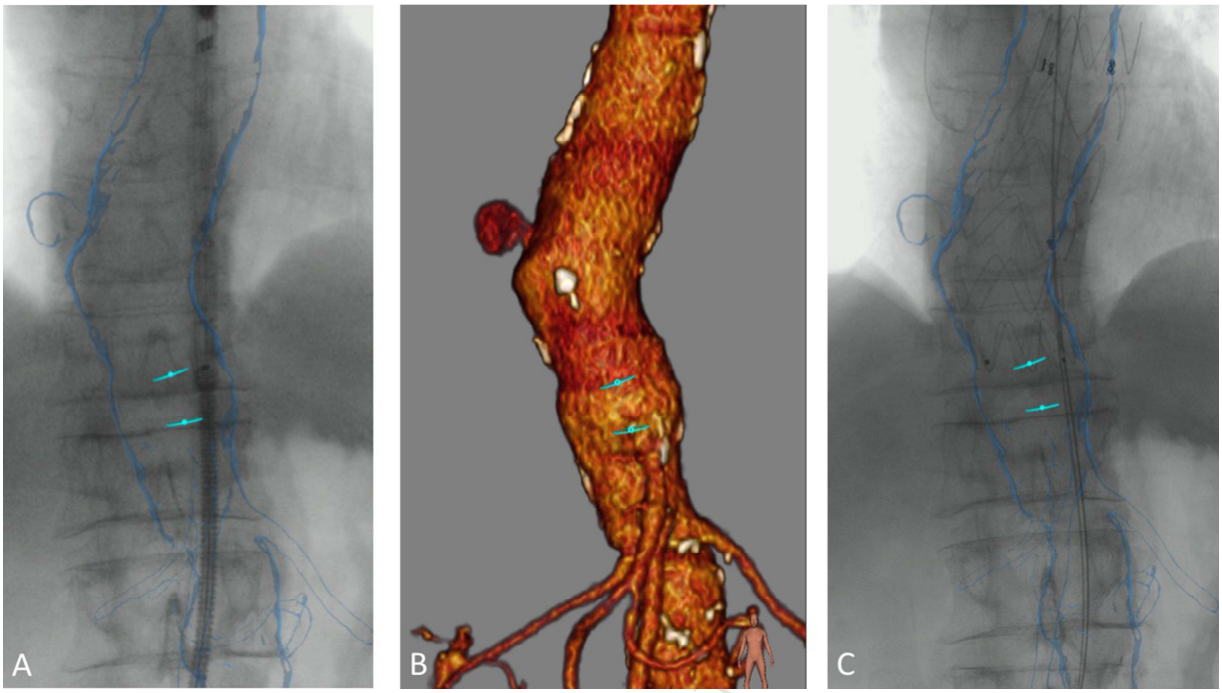

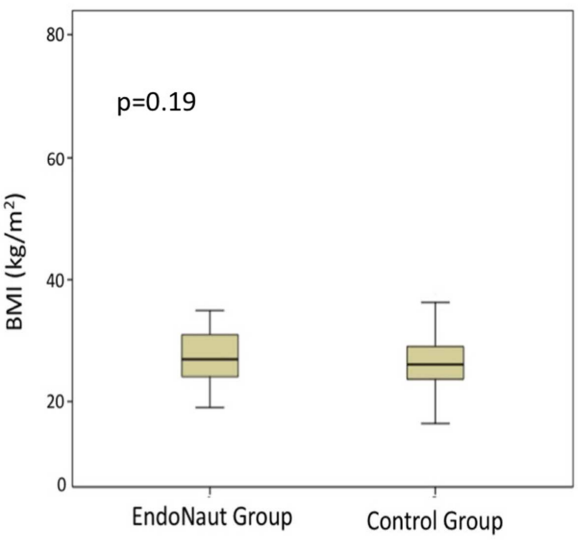
p=0.19
BMI (kg/m²)
80
60
40
20
0
EndoNaut Group
Control Group

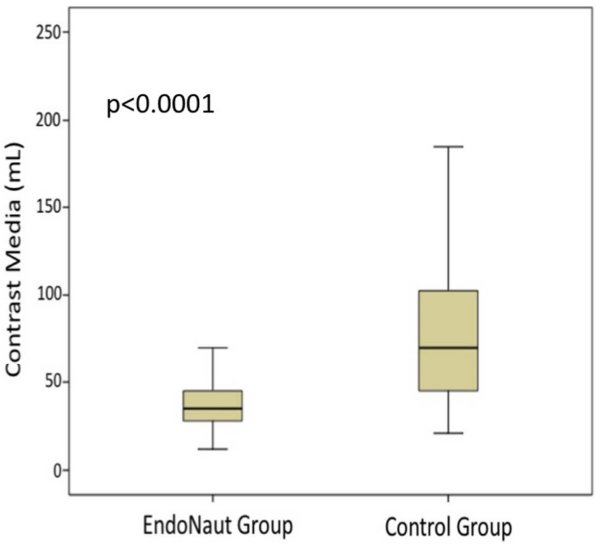
p<0.0001
Contrast Media (mL)
250
200
150
100
50
0
EndoNaut Group
Control Group

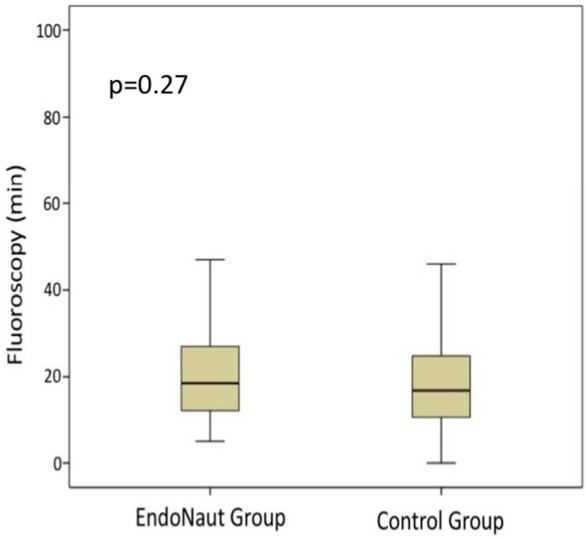
p=0.27
Fluoroscopy (min)
100
80
60
40
20
0
EndoNaut Group
Control Group

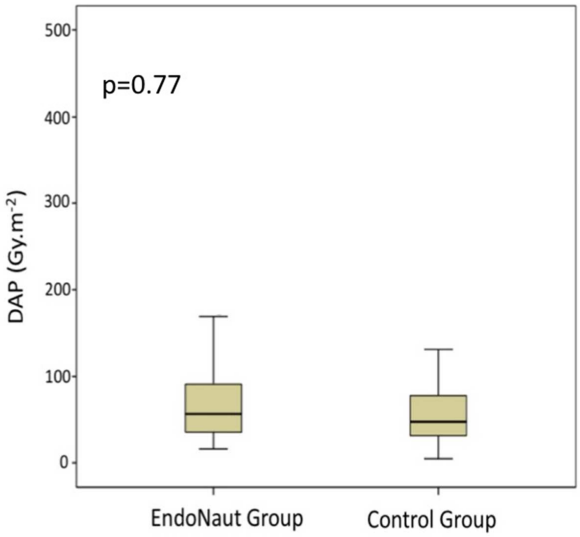
p=0.77
DAP (Gy.m⁻²)
500
400
300
200
100
0
EndoNaut Group
Control Group